AC and DC Percolative Conductivity of Single Wall Carbon Nanotube Polymer Composites

DAVID S. McLACHLAN,[1] COSMAS CHITEME,[1] CHEOL PARK,[2] KRISTOPHER E. WISE,[2]
SHARON E. LOWTHER,[3] PETER T. LILLEHEI,[3] EMILIE J. SIOCHI,[3] JOYCELYN S. HARRISON[3]

[1]School of Physics, University of the Witwatersrand, Johannesburg, South Africa

[2]National Institute of Aerospace, Hampton, Virginia

[3]Advanced Materials and Processing Branch, NASA Langley Research Center, Hampton, Virginia

ABSTRACT: The equations needed to correctly interpret both AC and DC conductivity results of single wall carbon nanotube (SWNT) polymer composites and the scaling of these results onto a single master curve are presented. Brief discussions on the factors that determine the critical volume fraction (ϕ_c) and the percolation exponent (t) are also given. The results for a series of SWNT–polyimide composites are presented and the parameters obtained from fitting these results are discussed. The critical volume fraction for electrical percolation of the present composite was about 0.0005. Results obtained from previous work on SWNT (MWNT)–polymer composites and other percolation systems and the modeling (interpretation) of these results are also discussed and compared. © 2005 Wiley Periodicals, Inc. J Polym Sci Part B: Polym Phys 43: 3273–3287, 2005

Keywords: carbon nanotube; conductivity; multifunctionality; nanocomposite; percolation; SWNT

INTRODUCTION

Future aerospace vehicles will require a significant reduction of mass, size of components, and power requirements, accompanied by an increase in the intelligence of these components. Single wall carbon nanotubes (SWNTs) are attractive for these applications because of their extraordinary combination of thermal, electrical, dielectric, and mechanical properties. Utilization of this suite of properties will enable radical design concepts of future vehicles based on multifunctional structural materials.

While a number of studies have reported successful mechanical reinforcement using SWNTs, few have attempted to take advantage of the sensing and actuating capabilities enhanced by SWNTs to achieve intrinsic multifunctionality in the nanocomposite. Recent results have shown that the electroactive response of a polymer can be enhanced by incorporating a small quantity of SWNTs, thereby improving its sensing capabilities.[1] Increasing the concentration of SWNTs enabled the polymer composites to be activated, in response to an applied electric field. This augmentation of the sensing and actuating capabilities of the polymer is directly related to the modified electrical and dielectric properties of SWNT polymer composite. Varying the SWNT concentration and orientation allow for tuning of the electrical, dielectric, and mechanical properties of the nanocomposites over a broad range. This tunable multifunctionality, in combination with the structural reinforcement of the nano-

composites, will enable the design of crucial intelligent and durable components for a variety of future aerospace vehicles.

This study focuses on understanding the electrical and dielectric properties of such composites within the framework of percolation theory. The intent of this work is to improve our ability to understand and design better composites incorporating SWNTs and to evaluate the utility of electrical measurements for use in nondestructive evaluation of such composites. The objective of the work presented here is to demonstrate the advantage of systematic incorporation of carbon nanotubes in structural nanocomposites to afford intrinsic multifunctionality. The scope of the work limits the definition of multifunctionality to structural materials capable of both sensing and actuating.

A brief review of percolation theory as it relates to this work is presented to clarify some inconsistencies in the literature in the application of percolation theory. Of particular interest are (1) the factors determining the critical volume fraction (ϕ_c), (2) the equations currently used to interpret both AC and DC conductivity (dielectric constant) results in percolation systems, and (3) how to scale such results onto a universal curve using only percolation equations. This section concludes with an outline of the current theoretical situation regarding the percolation exponent t, which is necessary because of some inconsistencies in the literature in the application of percolation theory. The next section describes the experimental procedures, and the one following it reports the current experimental results (AC and DC) and provides some discussion of the percolation parameters (ϕ_c, s, and t). This is followed by an extended discussion, together with some other DC experimental results and percolation parameters observed. In the last section, AC conductivity and dielectric results and the scaling of such results are discussed.

CRITICAL VOLUME FRACTION AND PERCOLATION EQUATIONS

The AC and DC conductivity of an extraordinarily large range of metal–insulator composites, as a function of volume fraction and frequency, can be described by the three standard percolation equations.[2,3] Alternatively, it has been shown that one may use the single equation,[4–7] given later, that incorporates the three standard per-

colation equations as special cases. The critical volume fraction (ϕ_c), at which the conducting inclusions first form a spanning cluster, has been observed to range from about 0.0005 (this study) to 0.56[6,8–10] for very different microstructures. The only common features in all these percolation systems are that the conducting component is randomly distributed and that intergranular resistances are present randomly between the conducting grains or regions.

For the case of randomly placed touching spheres on all 3D Bravais lattices, ϕ_c is found to be 0.16 in refs. 6, 8, 9, and references therein. The same value of ϕ_c is also found for completely random packing of conducting and insulating spheres of equal sizes as well as for randomly packed conducting and insulating similarly sized inclusions, even when the inclusions are far from spherical (graphite like flakes) and the conductivity is anisotropic.[4] Note that even in composites with anisotropic conductivity, ϕ_c is isotropic, as has been shown previously.[4] For cases where the insulating component tends to partially wet or coat the conducting grains,[10] ϕ_c can be higher than 0.16. This is also true, in principle, the insulating grains are much smaller than, and coat, the conducting grains.[11] When the radius of the conducting grains (R_c) is much smaller than the radius of the insulating ones (R_i), ϕ_c ranging between 0.012 and 0.065 (for $R_i/R_c = 8$–80) has been observed.[12] In the extreme case of $R_i/R_c = 100$ (ferrite powder on expanded polyurethane spheres), ϕ_c is 0.005.[13] This class of systems can be referred to as cellular systems.[12]

While much work has focused on spherical inclusions, other particle shapes have also been studied. For nearly spherical particles, such as carbon black, in a polymer, ϕ_cs well below 0.16 have been observed, indicating that the spatial distribution of the nearly spherical carbon particles is not truly random, for which case one would expect a ϕ_c of 0.16. It could be that the carbon is concentrated in 3D streaks or that the fine carbon particles coat and remain associated with the larger insulating polymer grains during preparation, thus giving rise to a cellular system as discussed earlier. Sintered materials, which start from roughly equal sized grains, tend to have a closed (nonpermeable) porosity when the porosity is about 0.03.[8] Therefore, if the conducting material is in the pores, ϕ_c would be about 0.03. As is discussed by Balberg,[14] low structure particles (*e.g.*, spheres), which have a low surface to volume ratio, lead to higher ϕ_cs than

high structure particles (*e.g.*, a mace head), which form percolation networks at lower ϕ's. For highly nonspherical particles such as sticks (fibers or bundles) or discs, ϕ_c can be very low. Currently, the most accurate theoretical approach for this class of system is based on the excluded volume concept.[15,16] A recent review of the application of the excluded volume approach to highly nonspherical carbon particles in polymer matrices is given by Celzard et al.[17]

For the randomly oriented SWNT–polyimide composite studied here, the degree of dispersion of the SWNTs is not known *a priori*. If the SWNTs are aggregated into bundles, one will have effective particles with a lower aspect ratio than individually dispersed SWNTs. We can, however, calculate upper and lower bounds for ϕ_c, using the equations for high aspect ratio sticks in 3D, as given in refs. 16 and 17. For example, if we assume an aspect ratio (length/diameter) of 20 (*e.g.*, $L = 3$ μm and $D = 150$ nm), we find a ϕ_c of about 0.05. If, on the other hand, we assume $L/D = 2000$ (*e.g.*, $L = 3$ μm and $D = 1.5$ nm; a single SWNT), ϕ_c is calculated to be about 0.0005, which is consistent with the experimental observations described later. This analysis is complicated by the fact that SWNT bundles contain an unknown number of tubes, which may result in the bundles being longer than 3 μm and having diameters greater that 1.5 nm but exhibiting a similar aspect ratio. In this case, the appropriate value of L/D is ambiguous, which leads to difficulty in predicting ϕ_c based on excluded volume theory alone. Calculations, based on the excluded volume theory in ref. 18, show that a 2.1 nm diameter bundle, consisting of 7 tubes, should have $\phi_c = 0.0007$, while a 3.5 nm bundle, consisting of 19 SWNTs, should have $\phi_c = 0.0012$. Further complications arise from the occurrence of single tubes bridging between adjacent bundles, which forms interbundle electrical contacts. This is an example of a highly structured "furry caterpillar" inclusion. It should also be noted that ϕ_c diminishes as the size distribution of percolating objects broadens.[19,20] Further discussion of the observed ϕ_c value of 0.0005 is given later.

For AC conductivity experiments discussed here, the composite conductivity (σ_m) is the sum of the real and imaginary conductivities, which is given by $\sigma_m = \sigma_{mr} + i\sigma_{mi}$. The conductivity of the SWNT is given by $\sigma_c = \sigma_{cr} + i\sigma_{ci}$ or simply $\sigma_c = \sigma_{cr}$ if ideal conductivity is assumed. For the insulating polymer $\sigma_i = \sigma_{ir} + i\sigma_{ii}$ where σ_{ii}

$= \omega\varepsilon_0\varepsilon_{ir}$, which may be approximated as $\sigma_i = i\omega\varepsilon_0\varepsilon_{ir}$ (ε_{ir} is the real part of the dielectric constant of the insulating component) if ideal lossless dielectric behavior is assumed for the polymer. In practice, σ_{ir} incorporates both the very small DC conductivity σ_{ir} and the dielectric polarization loss term $\omega\varepsilon_0\varepsilon_{ii}$. In all the reported AC percolation experiments, $\sigma_{cr} \gg \omega\varepsilon_0\varepsilon_{ir}$ or σ_{ci} (the imaginary part of the conductivity) for the conducting component and $\sigma_{ci} \ll \omega\varepsilon_0\varepsilon_{ii}$ (where ε_{ii} is the imaginary part of the dielectric constant of the insulating component). Because of this, ideal behavior for both the conductor and insulator is usually assumed.

In a recent series of studies,[4,5,7,12] it has been shown that the equation,

$$(1 - \phi)(\sigma_i^{1/s} - \sigma_m^{1/s})(\sigma_i^{1/s} + A\sigma_m^{1/s}) + \phi(\sigma_c^{1/t} - \sigma_m^{1/t})$$
$$\times (\sigma_c^{1/t} + A\sigma_m^{1/t}) \quad (1)$$

with $A = (1 - \phi_c)/\phi_c$ and s and t as exponents, best describes experimental results for percolation systems, especially the second order terms.[7,20] Above ϕ_c, σ_{mr} is the first order (larger in magnitude) and σ_{mi} is the second order (lower magnitude) term. Below ϕ_c, σ_{mi} ($\omega\varepsilon_0\varepsilon_{ir}$) $\ggg$ σ_{mr} for the frequencies used in most experiments, and the reverse is true. Note that the frequency dependence in this equation is determined solely by the dispersive properties of the components. When $s = t = 1$, the equation is equivalent to the Bruggeman symmetric media equation.[6,8] Equation 1 yields the two limits:

$$|\sigma_c| \rightarrow \infty : \sigma_m = \sigma_i \left(\frac{\phi_c}{(\phi_c - \phi)}\right)^s \quad \phi < \phi_c \quad (2)$$

$$|\sigma_i| \rightarrow 0 : \sigma_m = \sigma_c \left(\frac{(\phi - \phi_c)}{(1 - \phi)}\right)^t \quad \phi > \phi_c \quad (3)$$

These equations are the normalized standard percolation results[2,3] and characterize the exponents s and t. When $\omega\varepsilon_0\varepsilon_{ir} \gg \sigma_{ir}$, so that σ_i can be replaced by $\omega\varepsilon_0\varepsilon_{ir}$, eq 2 becomes

$$\varepsilon_{mr} = \varepsilon_{ir} \left(\frac{\phi_c}{(\phi_c - \phi)}\right)^s \quad \phi < \phi_c \quad (4)$$

This predicts a divergent ε_{mr} as ϕ approaches ϕ_c.[2,3] In reality, for $\phi > \phi_c$, ε_{mr} shows a frequency dependent peak as a function of ϕ where ε_{mr} is the second order term for $\phi > \phi_c$.[7,19,20] Recent measurements,[12] with $\phi < \phi_c$, fitted to

eq 4 have shown that s depends on the frequency at which the measurements were made and differs significantly from the s obtained from the DC measurements.

In the crossover region, where $\phi \cong \phi_c$ and which lies between $\phi - (\sigma_i/\sigma_c)^{1/(t+s)}$ or $(\omega\varepsilon_0\varepsilon_r/\sigma_c)^{1/(t+s)} < \phi$ and $< \phi + (\sigma_i/\sigma_c)^{1/(t+s)}$ or $(\omega\varepsilon_0\varepsilon_r/\sigma_c)^{1/(t+s)}$, eq 1 gives

$$\sigma_m \approx \sigma_i^{t/(s+t)}\sigma_c^{s/(s+t)} \quad \text{or} \quad (\omega\varepsilon_0\varepsilon_i)^{t/(s+t)}\sigma_c^{s/(s+t)} \quad (5)$$

which is in agreement with the theory given by Clerc et al.[2] and Bergman and Stroud.[3] Note that in the crossover region, no disagreement between eq 1 and the standard percolation equations has been observed experimentally, either in the first or second order.[7] Also note that eq 5 shows that in the crossover region, the conductivity σ_{mr} is proportional to $\omega^{t/(s+t)}$ and the dielectric constant ε_{mr} (note that $\varepsilon_m = \sigma_m/\omega\varepsilon_0$, ε_m is the dielectric constant of the composite) is proportional to $\omega^{s/(s+t)}$. These are the predicted and observed dispersion slopes, in slopes of log σ_{mr} against ω, at higher frequencies for percolation systems close to ϕ_c.[5] Equation 1 can be used to fit experimental AC results, as a function of ϕ and ω for all ϕ and ω, unlike eqs 2, 3, and 5 that only apply in restricted regions of ϕ and ω.

It is often possible to scale these types of experimental results onto a single master curve, as shown by refs. 5, 12, and references therein. The correct functions for two phase percolation systems, based on those given in refs. 2 and 3 and outlined in refs. 5 and 12, are as follows:

$$\sigma_m = \sigma_c\left(\frac{\phi_c - \phi}{\phi_c}\right)^t F_-(x_-) \quad \phi < \phi_c \quad (6a)$$

$$\sigma_m = \sigma_c\left(\frac{\phi - \phi_c}{1 - \phi_c}\right)^t F_+(x_+) \quad \phi > \phi_c \quad (6b)$$

where σ_m can come from either theoretical calculations or experimental results. The scaling functions $F_\pm(x_\pm)$ depend on the scaling parameters as follows:

$$x_- = \frac{\omega}{\omega_{c-}} = -\frac{\omega\varepsilon_0\varepsilon_i}{\sigma_c}\left(\frac{\phi_c - \phi}{\phi_c}\right)^{s+t} \quad (7a)$$

$$x_+ = \frac{\omega}{\omega_{c+}} = \frac{\omega\varepsilon_0\varepsilon_i}{\sigma_c}\left(\frac{\phi - \phi_c}{1 - \phi_c}\right)^{s+t} \quad (7b)$$

This shows that $\omega_{c+} = (\sigma_c/\varepsilon_0\varepsilon_i)((\phi - \phi_c)/(1 - \phi_c))^{s+t}$, from which it can be seen that ω_{c+} should be proportional to $\sigma_m(\phi, \omega = 0)^{(s+t)/t}$.

The aforementioned expressions for $\omega_{c\pm}$ assume a purely real σ_c ($\sigma_{ci} = 0$) and purely imaginary σ_i ($\sigma_{ii} = \omega\varepsilon_0\varepsilon_{ir}$). To ensure that curves drawn for $F_\pm$ fall on top of each other for different ϕ, the normalization employed in this study differs somewhat from the one used in refs. 2 and 3.

The predictions for the slopes of the scaling functions ReF_+, which is what is obtained from scaling σ_{mr} above ϕ_c, from standard percolation theory[2,3] and those obtained from eq 1,[5,12] are the same. Specifically, they are zero when ω/ω_{c+} and $\omega/\omega_{c-} < 1$ and $t/(s+t)$ for ω/ω_{c+} and $\omega/\omega_{c-} > 1$. In the previously defined crossover region, which now corresponds to ω/ω_{c+} and $\omega/\omega_{c-} \sim 1$, the plots exhibit curvature.

Scaling similar to that described earlier has also been observed in amorphous and other disordered systems, which are essentially one component media. As will be discussed later, this phenomenon can be interpreted in terms of a combination of percolation theory and hopping conductivity. The critical frequency ω_{c+} in this case depends on the nature and distribution of the hopping conductivity sites in the disordered material. These theories have also been incorrectly used to scale and model carbon nanotube–polymer systems, which are definitely two component percolation systems.

The universal value of exponent t (t_{un}), which is usually observed in computer simulations and for "ideal" systems, is 2.0.[2,3] Kogut and Straley[21] showed in computer simulations that if the low conductance bonds in the percolation network, or the intergranular conductances of the conducting component in a continuum system, have a very wide distribution, then t can be larger than t_{un}. This distribution can be due to a large range of effective geometrical resistivity factors in a continuous homogeneous conducting phase, such as those that occur in the Swiss Cheese (Random Void (RV)) model and the Inverse Swiss Cheese (Inverse Random Void (IRV)) model.[22,23] In the Swiss Cheese model, a range of very thin and highly resistive threads of conductor (cheese), between the large overlapping voids (air), give rise to a wide distribution in the conductances between the more extended or bulky regions of conductor. These models give values for t in the range 2.0–2.5. An extension to the RV model allowing still higher (apparently unlimited) values of t is given by Balberg.[24,25] The Links, Blobs, and Nodes model[26,27]

gives an upper limit of 2.35. Note that all of the aforementioned models assume a homogeneous (nongranular) conducting phase.

A model for granular conducting systems that gives rise to $t > t_{un}$ was proposed by Balberg.[24,25] This model is based on the dominant resistances in the current carrying Links and Blobs (now consisting of a granular conductor) being due to a large range of interparticle tunneling contacts, often through the polymer component. Chiteme et al.[28] proposed that the t values, considerably higher than 3 that were observed by several studies[4,12] are due to a combination of strictly geometrical effects (such as the highly resistive thin necks in the Swiss Cheese model[22,23]) and tunneling effects described in a model given in refs. 24 and 25. Unfortunately, no quantitative theoretical model for this situation has yet been attempted.

EXPERIMENTAL

A batch of purified HiPco SWNT was purchased from Carbon Nanotechnologies (Houston, TX). TEM and AFM microscopy along with Raman spectroscopy in radial breathing modes of HiPco SWNT revealed a diameter of $\sim$0.9–1.2 nm and a length of individual tubes of $\sim$3 μm.[29,30] An aromatic polyimide, (β-CN) APB/ODPA, was selected as a polymer matrix, and the chemical structure has been shown in ref. 31. The (β-CN)APB/ODPA was prepared from 2,6-bis(3-aminophenoxy) benzonitrile ((β-CN)APB) and 4,4′-oxidiphthalic anhydride (ODPA) in N,N-dimethylacetamide (DMAc) via a poly(amic acid) solution.

A dilute SWNT solution, typically about 0.05 wt % in DMAc, was prepared by homogenizing for 10 min (750 rpm with a 6 mm diameter rotor homogenizer) and sonicating for an hour at 47 kHz. The sonicated SWNT solution was used as a solvent for the poly(amic acid) synthesis with the diamine and dianhydride. The entire reaction was carried out with stirring in a nitrogen-purged flask immersed in a 40 kHz ultrasonic bath until the solution viscosity increased and stabilized. Sonication was ceased and stirring was continued for several hours to form a SWNT–poly(amic acid) solution.

A series of SWNT–polyimide composite films were prepared with a SWNT concentration of 0, 0.02, 0.035, 0.075, 0.1, 0.2, 0.5, 1.0, 2.0, and 5.0 wt %. The SWNT–poly(amic acid) solution prepared was cast onto a glass plate and dried in a dry air-flowing chamber. Subsequently, the dried tack-free film was thermally imidized in a nitrogen-circulating oven to obtain a solvent-free freestanding SWNT–polyimide film.

As the films prepared were 50–70 μm thick, this suggests that the films cross sections had the equivalent of about 20 nanotubes, laid end to end. Therefore, one can justify analyzing the transverse results in terms of 3D percolation theory. If a film is less than 10 conducting particles thick in their elongated direction, one cannot be confident that it is a 3D system in a percolation sense.

Good electrical contact to the composites was ensured by first sputtering a thin (20 nm) coating of gold over the selected area and then painting this area with silver paste, into which copper wires were embedded. The DC conductivities were measured using a Keithley 917 Electrometer in the V/I mode, and the AC properties were measured using a Novocontrol Broadband Dielectric Spectrometer. Scanning electron microscopy (SEM) images of the cryogenically fractured surfaces were taken with a Hitachi S-5200 field emission SEM (FE-SEM).

RESULTS

The DC results will be discussed first because for the best and most reliable results, the critical volume fraction ϕ_c must be determined by DC resistivity measurements using either eq 1 or eqs 2 and 3, with a common ϕ_c and eliminating any experimental points that lie in the crossover region. If AC measurements are used, there can be effects due to the dielectric conductivity ($\omega\varepsilon_0\varepsilon_r$). (In ref. 10, it was shown that the result for ϕ_c was the same, within experimental error, from DC measurements and from an examination of the superconducting intergranular tunneling results.) In the present study, the transverse DC conductivity measurements (perpendicular to the plane of the film) were fitted using eq 1 as shown in Figure 1. The results of this fit are $\phi_c = 0.000500$, $s = 0.797 \pm 1.012$, $t = 2.77 \pm 0.24$, $\sigma_i = 10^{-16.26\pm0.13}$ S/cm, and $\sigma_c = 10^{1.95 \pm 0.59}$ S/cm. The results below ϕ_c, including the value for s (the error in the parameters s is larger than the corresponding s value), were not very reliable, as there were only a few points, the measurements were made near the limits of the Keithley 617, and the dominant
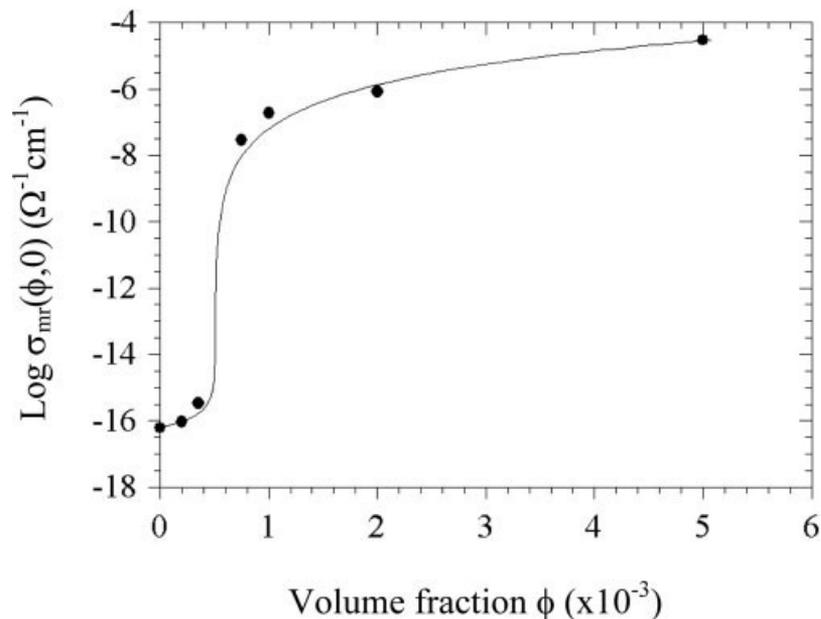
Figure 1. DC experimental conductivity results and the fit obtained using eq 1, plotted as the log of the transverse conductivity against the volume fraction of SWNTs.

resistivity of the polyimide might vary. Note that in the aforementioned fitting, the value of ϕ_c was fixed at 0.0005 (which gave the least error when ϕ_c was varied from 0.00047 to 0.00053) while the other parameters were left free. Using eq 3 and the samples with ϕ from 0.00075 to 0.05 (there are no points in the crossover region), the fitted parameters are $\phi_c = 0.000506 \pm 0.000045$, $t = 2.22 \pm 0.10$, and $\sigma_c = 10^{0.51 \pm 0.05}$ S/cm.

It was not possible to make resistivity measurements below ϕ_c in the longitudinal direction (along the plane of the film), as the resistivity was too high. The longitudinal results, shown in Figure 2, are fitted using eq 3 with the following parameters $\phi_c = 0.000555$, $t = 2.21$, and $\sigma_c = 10^{1.71}$ S/cm (the 0.00075 point was inconsistent and is not incorporated). From these results, it can be observed that ϕ_c is reasonably similar in both directions, demonstrating that the conductivity of the SWNT component of the composite was not very different in the transverse and longitudinal directions, which suggests uniform dispersion of SWNTs throughout the matrix. Note that previously published data on SWNT "bucky" paper[32] gives a σ_c in the range 10^2–10^3 S/cm, which is in reasonable agreement with the above results, especially considering that all results have to be extrapolated from a low ϕ value to 1.

As both the t values obtained using eq 3 are not much greater than 2, using the arguments

given at the end of the previous section, it can be concluded that the range of inter SWNT resistivities (the bundles must contact along the percolation path at one or more SWNTs) is not large or that a percolation path through inter SWNT contacts, with a fairly constant resistivities, is the dominant one.

The measured t value does not indicate whether the SWNT bundles are coated with a polymer layer or not. However, it does indicate that, if it exists, the thickness of any coating layer between the SWNTs or the bundles is very uniform, as a wide range of coating thicknesses (tunneling barriers) should lead to a higher t value. In actual fact, this polymer showed good wetting on the surface of SWNT according to energy loss spectroscopy[29] because the interaction was reinforced by donor–acceptor charge transfer interaction.[31] This good adhesion provides a uniform dispersion, but may prevent direct SWNT–SWNT (carbon–carbon) contacts. This may explain the good dispersion and low percolation thresholds, but relatively low conductivity above ϕ_c and the low extrapolated value at $\phi = 1$. Energy filtered transmission electron microscopy (EFTEM) observations[29] show a uniform polymer layer coating on a 2-nm thick coated SWNT, which indicated that the layer is as thin as 5 Å, yielding moderately low and reasonably uniform resistance tunnel barriers.
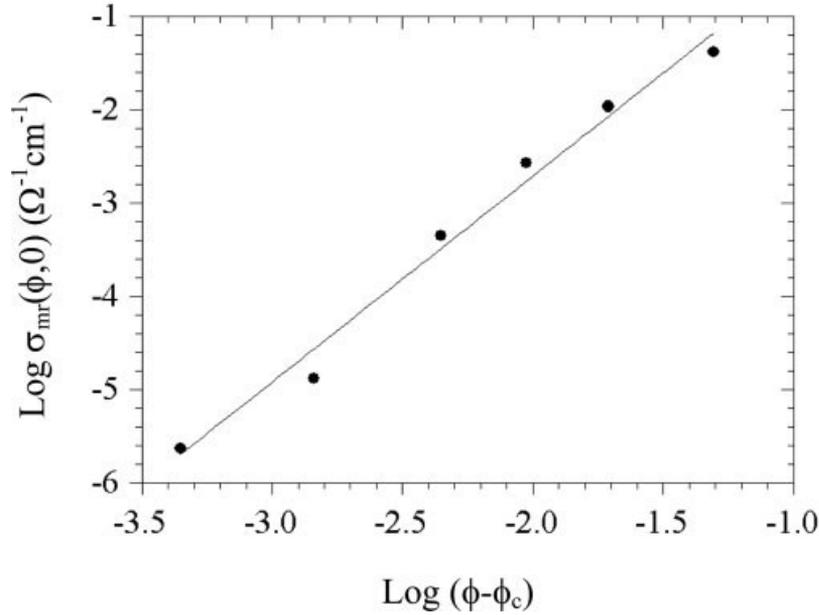
Figure 2. DC experimental conductivity results and the fit obtained using eq 3, plotted as the log of the longitudinal conductivity against log $(\phi - \phi_c)$.

Unfortunately, other than the results in refs. 5 and 12, there are few DC measurements of s. As ref. 12 clearly shows, from dielectric measurements using eq 2, the value of s decreases with the increasing frequency. This frequency dependence has not been previously observed and no theory exists that addresses this problem. Therefore all that can be said of the currently observed s value is that it is a "typical" experimental value as seen in refs. in 5, 12 and the references therein, and lies close to the universal value of 0.87.

It is very difficult to explain the observed ϕ_c, as the exact morphology of the SWNT bundles is not known. High-resolution scanning electron micrographs shown in Figure 3(a) revealed that SWNTs dispersed in the polymer matrix uniformly through the film thickness in 3D on a nanometer scale. Figure 3(b) shows exposed SWNTs on the fracture surface at high magnification, which clearly shows flexible SWNTs running out of the polymer matrix, with multiple branches still embedded in the matrix. All of the visible SWNTs are seen to have high aspect ratios. Physical entanglements of the SWNTs were also often seen. Therefore, it can be safely assumed that the composite is macroscopically uniform with conducting inclusions (SWNT bundles) randomly, but homogeneously, distributed in 3D. There are several factors influencing the percolation threshold ϕ_c, which might include some or all of the following:

1. The high aspect ratio of inclusions [Fig. 3(b)], the SWNTs, and SWNT bundles in the present system gives rise to a ϕ_c value, which can be easily understood by the excluded volume model. Unfortunately, the mean size and distribution of the aspect ratios of the experimentally observed bundles are not known. A L/D of 2000 is necessary to give the observed threshold of 0.0005 (correct for a single SWNT). However, as a bundle of only 19 SWNTs gives a ϕ_c of 0.00117, other factors must be contributing to the low ϕ_c.

2. Because of the different lengths of the SWNTs and the irregular packing of the nanotubes, the bundles have an irregular surface that gives a higher structure factor than a smooth stick. These high structure SWNT bundles were shown in Figure 3, with multiple branches and entanglements with neighboring tubes. Higher structure factors lead to lower ϕ_c values.

3. SWNT bundles are small inclusions with a very high surface area, which can reach 2000 m^2/g. For the same volume fraction, small inclusions must lie close together and have a larger amount of surface area in close proximity than larger particles. This leads to a greater probability of conductive tunneling between the bundles. This "size"
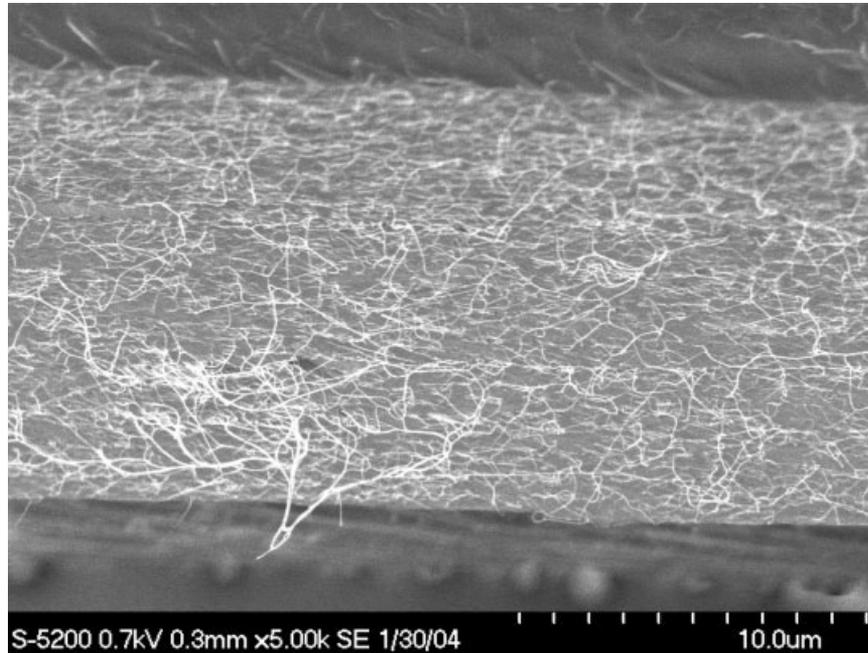
(a)
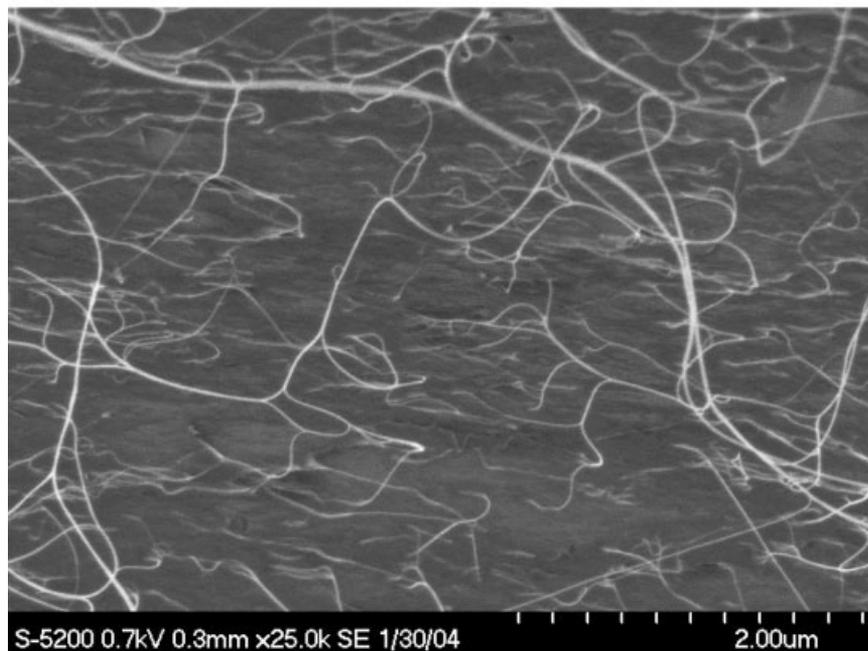
(b)

Figure 3. HRSEM of 0.5 wt % SWNT/polyimide composite (fracture surface) (a) cross section view of the composite film and (b) higher magnification of (a).

effect, which is probably only important where the conducting particles have 2 or 3 dimensions below 10 nm, is not taken into account in classical percolation theory, and will lead to a lower measured ϕ_c.

4. The SWNT bundles and especially isolated SWNTs or SWNTs protruding from the bundles are very flexible as seen in Figure 3(b), which limits the applicability of rigid stick excluded volume fraction models.
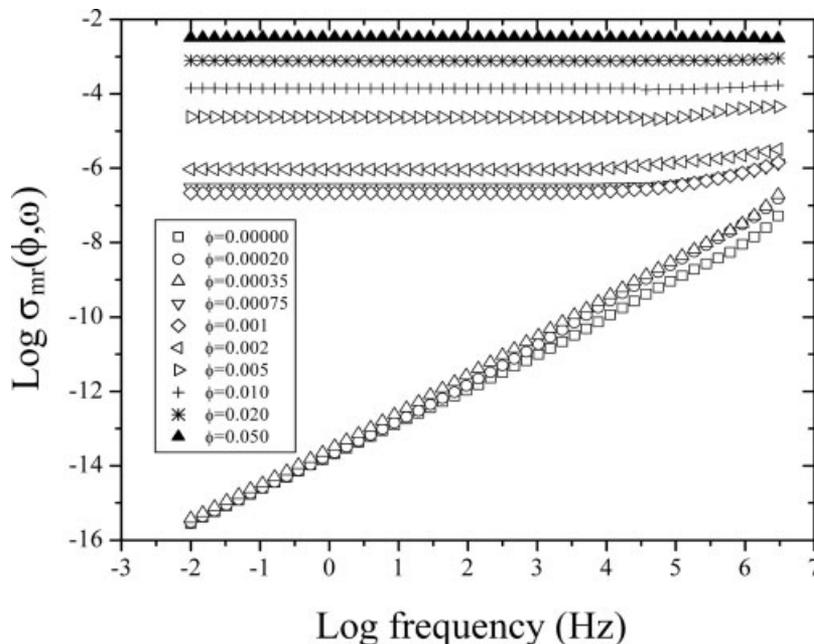
Figure 4. Log of the real AC conductivity (σ_{mr}) plotted against the log of the frequency, for various ϕ values, the symbols for which are given in the figure.

More importantly, if there are physical entanglements and small attractive forces that hold contacting neighboring SWNTs together, then ϕ_c will be markedly lowered. These contacts can be either between the isolated SWNTs or the SWNTs protruding from the bundle surfaces or combinations of these, and the contacts can be with or without a tunneling barrier.

While (1) appears to be the major factor, it is not by itself sufficient, and therefore some or all of the other three factors are also playing a role in determining the observed ϕ_c of 0.0005.

The longitudinal and transverse conductivity results showed that these composites are reasonably isotropic in both the directions. The slightly lower conductivity in the transverse direction is possibly due to the thin resin rich layer on both sides of the film. Note that this good dispersion was achieved by donor–acceptor interaction between electron withdrawing functional groups (nitrile) of the aromatic polyimide matrix and the extended sp^2 hybrid orbitals of the SWNT surfaces. This interaction was verified by an upshift of the tangential mode peak of the SWNTs in Raman scattering and a downshift of nitrile group of the polyimide in FTIR spectra.[31]

The log of the AC conductivity, as a function of the log of the frequency, is shown in Figure 4.

For samples just above ϕ_c, the conductivity is initially constant and then starts to increase at higher frequencies (about 3.5 kHz for the 0.00075 sample). The available frequencies are not high enough for the slopes of the curves to be linear and approach a constant slope as is often observed. A slope of $t/(s + t)$, about 0.75, is predicted by percolation theory (eq 5), but not always observed.[12] Below ϕ_c, the slopes of the conductivity curves are roughly linear with a slope in the range of 0.9–1.0, which is commonly observed for a wide range of highly resistive materials but not well understood.[33] The clear difference in the dispersion curves above and below ϕ_c allows one to distinguish between conducting samples and dielectric samples. Therefore, Figure 4 shows that the percolation threshold lies between 0.00035 and 0.00075, consistent with the DC results.

Plots of the log of the dielectric constant against the log of the frequency are given in Figure 5. At fixed frequencies, the dielectric constant increases slowly with ϕ (more noticeable at lower frequencies) up to ϕ_c (eq 4) and then more rapidly at and above ϕ_c. There is no dispersion for low ϕ samples, but a small negative slope for the samples just below ϕ_c, as predicted by percolation theory (eq 5), can be seen on an expanded scale. This dispersion can be much more clearly seen in the experimental results
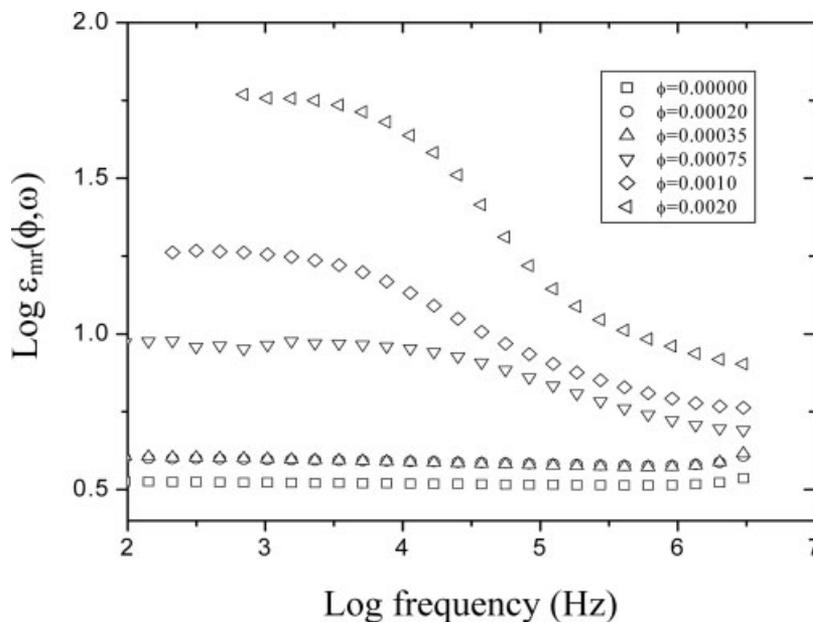
Figure 5. Log of the real AC dielectric constant (ε_{mr}) plotted against the log of the frequency, for various ϕ values, the symbols for which are given in the figure.

given in refs. 5 and 12. Dielectric properties with ϕ above 0.002 could not be measured reliably because of the high conductivity of the samples. These results also indicate that the percolation threshold lies between 0.00035 and 0.00075.

A Cole–Cole plot (imaginary impedance against real impedance) for the $\phi = 0.002$ sample is given in Figure 6. The characteristic, or peak, frequency f_c for each arc is given by $\sigma_{mr}/2\pi\omega_0\varepsilon_{mr}$ for the material or component giving rise to the arc. For low ϕ (below 0.00075) samples, there are no arcs, while for the 0.00075 sample, the arc is not complete as σ_{mr} is too low. The 0.001 and 0.005 samples gave the usual depressed semicircular arc with a ϕ_c, or peak frequency, of 37.5 kHz and 274 kHz, respectively, indicating a homogeneous material. The slight double hump structure (hump peaks at 37.5 and 274 kHz) for the impedance arc of the 0.002 sample might indicate that it is slightly inhomogeneous. Therefore, impedance measurements may monitor homogeneity in this type of material but only over a very limited range of composition, because of the limited frequency range of currently available instrumentation.

Figure 7 shows a plot of log ε_{mr} against ϕ, which clearly illustrates that the dielectric constant continues to increase through and beyond ϕ_c. Dielectric measurements cannot be made on conducting samples at very low frequencies, hence the restricted frequency range. Note that

the variation of ε_{mr} with frequency (at high ϕ) is consistent with both eq 1 and previous experiments.[19,20] The increase in ε_{mr} with increasing ϕ below ϕ_c, predicted by eqs 1 and 4, can easily be observed if the results are plotted on a different scale. It is likely that the high dielectric constant comes from very small distances between some conducting clusters. However, these capacitances are shorted by other contacting clusters, which form a DC continuous network.

DISCUSSION

DC Results

In previous work[34–36] on the DC conductivity of SWNT–polymer and MWNT–polymer composites, the DC conductivity results above ϕ_c were analyzed using the version of eq 3, found in refs. 2 and 3. These analyses, however, do not allow for the correct identification of ϕ_c, because of the unspecified arbitrary constant. Also no measurements of the conductivity were made below ϕ_c, which meant that the exponent s could not even be estimated and, as previously stated, unambiguous values of ϕ_c require fitting using eq 1 or eqs 2 and 3, with a common ϕ_c. However, as the transition is extremely sharp in all these experiments, the values of ϕ_c are probably reliable. The parameters obtained in the present experi-
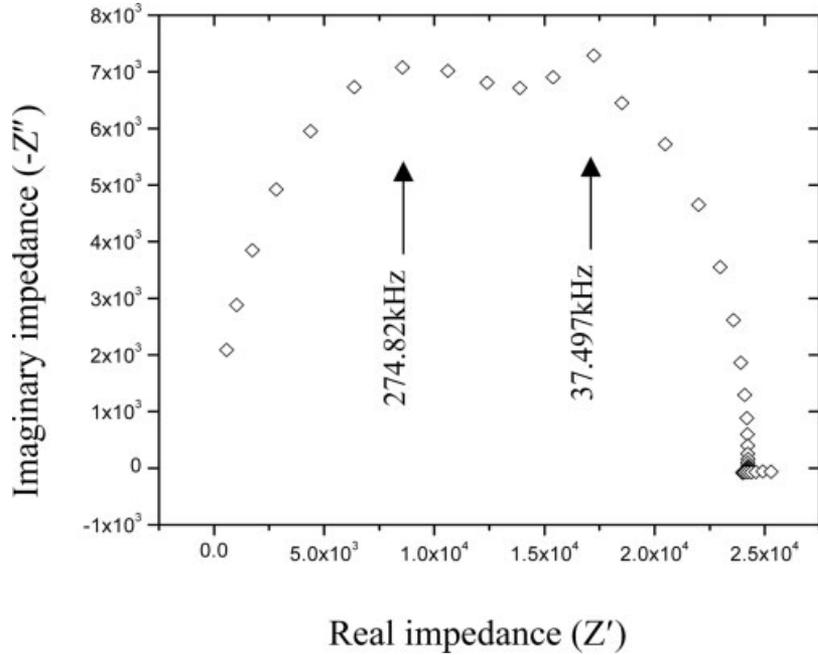
Figure 6. Plot of the imaginary impedance against the real impedance (Cole–Cole plot) for the $\phi = 0.002$ sample.

ments and refs. 34–36 are summarized in Table 1. Note that only in the present work is the conductivity measured in two nonequivalent directions and those measured refs. 34–36 were made only in one direction. Also note that the films in ref. 34 are only 80 nm thick and the nanotubes or bun-
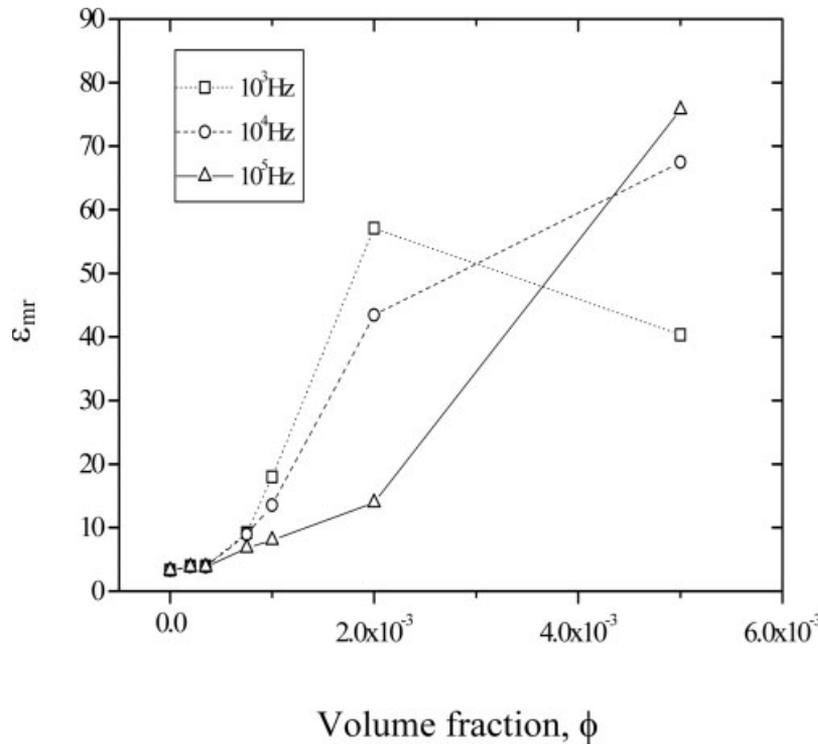

Figure 7. Log of the AC dielectric constant (ε_{mr} below ϕ_c and ε_{mi} above ϕ_c) plotted against the log of the frequency, for various ϕ values, the symbols for which are given in the Figure.

Table 1.   Parameters Obtained in the Present Experiments and Refs. 34–36

Polymer	Dispersion	ϕ_c	t	s	σ_c (S/cm)	σ_i (S/cm)
Polyimide	Shear	0.0005 (T)	2.77	0.797	8.9×10^1	6.3×10^{-17}
(present study)	Sonication	0.000506 (T)	2.22	–	3.2×10^0	–
	In-situ polymerization	0.000555 (L)	2.21	–	5.1×10^1	–
PVA (ref. 34)	Sonication spin casting	0.00029	1.36	–	2×10^{-5}	$\approx 10^{-12}$
Epoxy (ref. 35)	Shear phase separation	0.000025	1.2	–	2×10^0	$\approx 10^{-11}$
Epoxy (ref. 36)	Shear *in-situ* polymerization	0.003	1.44	–	7×10^{-4}	$\approx 10^{-16}$

dles lengths are certainly larger than 80 nm. Therefore, the films do not contain sufficient randomly oriented nanotubes in the transverse direction, which is also the direction of measurement, to be a valid 3D percolation system. The reason why no samples with PmPV (poly(*m*-phenylene-vinylene-*co*-2,5-dioctyloxyp-phenylenevinylene)) as the polymer were studied below the percolation threshold could be that a few of the single bundles or fibers were sufficiently long and oriented so as to provide a short circuit between the electrodes. Note that only the results with PVA (poly (vinyl alcohol)) as the polymer are quoted for ref. 34 in Table 1.

The ϕ_c value range is as follows: 0.000025 (high shear stirring and phase separation[35]), 0.00029 (sonication and spin coating[34]), 0.0005 (*in situ* polymerization under sonication and shear (present study)), and 0.003 (high shear mixing during polymerization[36]). Note that all of the above ϕ_cs, except the last, are in the range to be expected for a composite made up entirely of only single (*i.e.* nonbundled) SWNTs and MWNTs, only if excluded volume theory is used. As all of the SWNTs and MWNTs occur in bundles, with far lower *L/D* ratios, all the lower of ϕ_cs must also, in part, be due to some or all of the factors discussed in the previous section.

The values of t obtained from refs. 34–36 are all below the universal value of t_{un} and therefore not compatible with any of the theories given earlier. Although 3D t values of less than 2 have been previously observed (for instance one of the seven systems studied in ref. 12), no definitive explanation exists. The reasons advanced for low values of t in 3D include nonstatistical (nonrandom) distribution of bundles or clusters (*e.g.*, phase separation in ref. 35), as well as changes in the proportion of dead ends along the percolation path. As in true 2D systems, the universal values of s and t are the same and lie between 1.2 and 1.36, and there is also the possibility that within the 3D system,

there is a 2D system that (partially) controls the conductivity.[37] In this case, it is likely that the percolation parameters measured in two nonequivalent directions should be different. This is more likely to be in the s and t values, as ϕ_c value must be the same in all directions, except for a 3D-layered system with electrically isolated 2D layers. (Only if the occasional contact exists between the layers, ϕ_c is then isotropic.) Unfortunately, measurements in two directions were not performed in refs. 34–36. Note that in the clearly defined, but virtually impossible to achieve, geometry[6,9] for the Bruggeman Symmetric Media, Maxwell's equations rigorously give a t of one in 3D. Also note that if the films or other samples studied are less than 10 times, the longest dimension of the conducting particles thickens, in the direction of the current, and the sample cannot be assumed to be a true or standard percolation system. Therefore, in ref. 34, even if the percolation equations can model the data, one cannot expect to get understandable percolation parameters. One last point to note is that, if the values of t are less than 2.0, the models discussed earlier are not immediately applicable. However, it is probably safe to assume that if the range of inter nanotube bundle resistivities is not too large, or according to the mechanisms proposed by Kogut and Straley[21] and Balberg,[24,25] the observed values of t should be higher.

The values of σ_c, obtained from the extrapolation of the plots of $\sigma_m = \sigma_c((\phi - \phi_c)^t/(1 - \phi_c)^t)$ (eq 3), are listed in Table 1. The extrapolated values listed in refs. 34–36, which used the equation $\sigma_m = C\sigma_c(\phi - \phi_c)^t$, $\phi > \phi_c$, where C is an arbitrary constant, are also included. Note that in these particular cases as $(1 - \phi_c)^t$ is very close to 1, no corrections have to be made to their σ_c values. The results seem to fall into two categories, the present work and that of ref. 35 giving a σ_c lying in the range 2.0–89 S/cm and the results from refs. 34 and 36 lying in the range $0.2 \times 10^{-4} - 7 \times 10^{-4}$ S/cm.

AC Results and Scaling

At low frequencies, there is a very strong similarity between the plots of log σ_{mr} against log frequency as given in Figure 4 and similar plots in refs. 34–36. After an examination of refs. 5, 12, 34, and 36, it is immediately apparent that, if the present measurements could have been made at higher frequencies, the present results would not only have had the upturn at ω_c but also have had a straight line region at higher frequencies. Therefore, the present results are not really suitable to illustrate scaling, but subsequent measurements on these systems have shown such behavior at temperatures above 50 °C.[38]

The results in refs. 34 and 36, for $\phi > \phi_c$, are scaled onto a single "master curve" by dividing by the DC or low frequency conductivity and then sliding the resultant curves along the log $(\sigma(\omega)/\sigma(0)) = 0$ axis, by a factor $(1/\omega_c)$, until they coincided. A criterion that is often used is that at ω/ω_c, $(\sigma(\omega)/\sigma(0))$ should equal 1.1. Similar scaling onto a master curve has been done in refs. 5, 12, and references therein. The equation, for the conductivity as a function of frequency, used to interpret the results in ref. 34 is $\sigma(\omega) = \sigma_0$ i.e. $(\sigma(\omega = 0)) + k\sigma_c (\omega/\omega_c)^s$, but was developed for homogeneous one- and two-phase systems and does not strictly apply to percolation systems, with a distinct conducting and insulating phase. This model is called the extended pair approximation, where k is an arbitrary constant and the s is not related to the percolation exponent in eqs 1 and 2. In ref. 36, the mathematically equivalent equation to the one above for $\sigma(\omega) = \sigma_c$ i.e. $(\sigma(\omega = 0)) + A(\omega)^s$, which is the universal dielectric response equation,[33] was used, but it is obviously the same as the previous one, with somewhat different definitions of the parameters, with A again being an arbitrary constant. Ref. 39 shows how universal AC conduction equations can model the temperature dependence of nominally homogeneous systems like glasses, melts, doped polymers, amorphous films, and polycrystalline diamond. The only two-phase system discussed in ref. 39 was the polycrystalline diamond, which has a grain boundary phase. Therefore, this equation also does not strictly apply to percolation systems. Hunt[40] describes this phenomenon in terms of percolation theory and hopping conductivity. The critical frequency (ω_{c+}) is in this case dependent on the nature and distribution of the hopping conductivity sites in the disordered material. In refs. 5, 12 and the references therein, the experimental results were scaled onto a master curve and the curve modeled using either eq 5 (see also ref. 2 and 3) to analyze the slope of the straight line region only or the entire curve using eq 1.[5,12] Note that in ref. 41, it was shown that a single carbon black-polyethylene system could be scaled onto a master curve when the temperature (i.e. σ_i/σ_c) was varied, as is to be expected from an examination of eqs 6 and 7.

In both the equations in the previous paragraph, a crucial parameter is $\omega_c(\omega_0)$, the angular frequency, which indicates where the conductivity results deviate from zero slope, and is proportional to $(\phi - \phi_c)^x$ or $(p - p_c)^x$. (Here p is the probability of a particular site being occupied by a conductor and p_c the critical probability.) This is shown to be the case by means of plots of ω_c against $p - p_c$ in refs. 33 and 35. This is of course related to the DC conductivity of their systems, and so these results give $\omega_c(\omega_0)$ values, which are linear functions of the DC conductivity. There is no contradiction between this dependence and the percolation approach, as eq 7 shows that $\omega_c(\omega_{c+})$ should also be proportional to σ_m. These relationships have also been tested for a number of systems in refs. 5, 12, 41, and the references therein.

As data, which shows a significant enough increase in the conductivity at high frequencies, were not obtained in this work, scaled data for a carbon black-talc system were fitted and used in the following argument. Figures 8(a) and (b) show that both the equations given in the above two paragraphs, which do not include the concept of a percolation threshold, and eqs 1, 6, and 7 can be fitted to scaled data plots of the log of the normalized conductivity against normalized frequency. These curves are very similar and by a suitable choice of parameters can be made to agree with the data at the lowest and highest frequencies.

CONCLUSIONS

One conclusion that can be made from the series of studies[3,4,6,11,12,20,40] is that, while the experimental results nearly always agree with the predictions of eqs 1–5 and can be scaled onto a master curve, as expected from eqs 1, 6, and 7, the exponents s and t as well as the experimental ω_c values are not always self consistent or
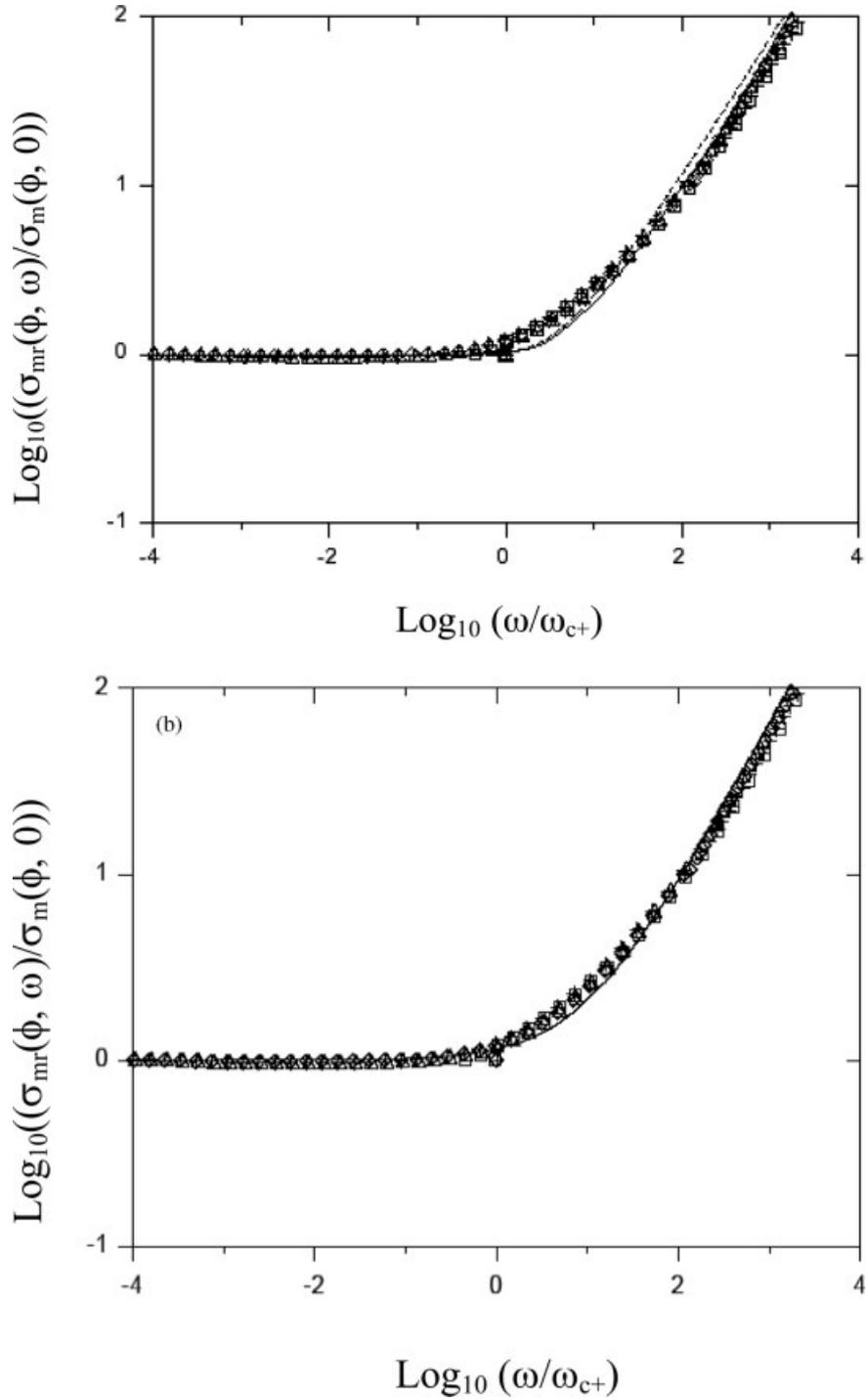
Figure 8. (a) Log–log plot of the scaled AC conductivity *vs.* scaled frequency for the carbon black-talc system for samples $\phi = 0.01291$ ($\square$), $\phi = 0.01343$ (Δ), $\phi = 0.01351$ ($\diamond$), and $\phi = 0.01334$ (+). The solid line is a best fit to eq 1, with a free range parameter: $s'' = 0.48 \pm 0.04$ and $t = 2.26 \pm 0.20$, which gives a $t/(s'' + t) = 0.82$. The fit of the DC data to the phenomenological equation gave the parameters: $\phi_c = 0.0131 \pm 0.0006$, $s = 0.90 \pm 0.20$, and $t = 2.26 \pm 0.11$, which gave $t/(s + t) = 0.72$. When these parameters are used, the theoretical fit is not at all satisfactory. When $s' = 0.43 \pm 0.03$, the exponent from dielectric measurements (eq 4) at 1 kHz is used, $t/(s + t) = 0.84$ and the fit (dashed line) is obviously better as this value is much closer to the best fit parameters. However, there is the noticeable deviation at high frequency. (b) log–log plot of the scaled AC conductivity *vs.* scaled frequency for the carbon black-talc system for samples $\phi = 0.01291$ ($\square$), $\phi = 0.01343$ (Δ), $\phi = 0.01351$ ($\diamond$), and $\phi = 0.01334$ (+). The solid line is a best fit to the universal equation: $\frac{\sigma_{mr}(\phi, \omega)}{\sigma_m(\phi, 0)} = 1 + k(\frac{\omega}{\omega_c})^x$, with the parameters: k = 0.145 ± 0.004 and $x = 0.880 \pm 0.003$.

even very well understood. It would appear that the same is true for nanotube–polymer systems, which have the lowest ϕ_c values of any system. It can only be hoped that our understanding of the factors determining s and t, and to a lesser extent ϕ_c, improves by employing appropriate equations in further studies of well-dispersed nanotube–polymer and other systems.

REFERENCES AND NOTES

1. Ounaies, Z.; Barnes, C.; Park, C.; Harrison, J. S.; Lillehei, P. T. Submitted for publication.
2. Clerc, J. P.; Girand, G.; Langier, J. M.; Luck, J. M. Adv Phys 1999, 39, 191.
3. Bergman, D. J.; Stroud, D. Solid State Physics; Academic Press: San Diego, California, 1992; Vol. 46, p 147.
4. Wu, J.; McLachlan, D. S. Phys Rev B 1997, 56, 1238.
5. Wu, J.; McLachlan, D. S. Phys Rev B 1998, 58, 14880.
6. McLachlan, D. S. J Electroceramics 2000, 5, 93.
7. (a) McLachlan, D. S.; Chiteme C.; Heiss, W. D.; Wu, J. Phys B: Condens Matter 2003, 338, 256; (b) McLachlan, D. S.; Chiteme C.; Heiss, W. D.; Wu, J. Phys B: Condens Matter 2003, 338, 261.
8. McLachlan, D. S.; Blaszkiewics, M.; Newnham, R. E. J Am Ceram Soc 1990, 73, 2187.
9. McLachlan, D. S. In MRS Proceedings, Pittsburgh, Pennsylvania, 1996; Vol. 411, p 309.
10. McLachlan, D. S.; Rosenbaum, R.; Albers, A.; Eytan, G.; Grammatika, N.; Hurwitz, G.; Pickup, J. Zallen, E. J Phys: Condens Matter 1993, 5, 4829.
11. Kusy, R. P. J Appl Phys 1997, 48, 5301.
12. Chiteme C.; McLachlan, D. S. Phys Rev B 2003, 67, 024206.
13. Chiteme C.; McLachlan, D. S. Private communication.
14. Balberg, I. Phys Rev Lett 1987, 59, 1305.
15. Balberg, I.; Anderson, C. H.; Alexander, S.; Wagner, N. Phys Rev B 1984, 30, 3933.
16. Balberg, I. Philos Mag B 1987, 56, 991.
17. Celzard, A.; McRae, E.; Deleuse, C.; Dufort, M.; Furdin G.; Marche, J. F. Phys Rev B 1996, 53, 6209.
18. Ounaies, Z.; Park, C.; Wise, K. E.; Siochi, E. J.; Harrison, J. S. Compos Sci Technol 2003, 63, 1637.
19. McLachlan, D. S.; Heiss, W. D.; Chiteme, C.; Wu, J. Phys Rev B 1998, 58, 13558.
20. Heiss, W. D.; McLachlan, D. S.; Chiteme, C. Phys Rev B 2000, 62, 4196.
21. Kogut, P. M.; Straley, J. P. J Phys C: Solid State Phys 1979, 12, 2151.
22. Halperin, B. I.; Feng, S.; Sen, P. Phys Rev Lett 1985, 54, 239.
23. Feng, S.; Halperin, B. I.; Sen, P. Phys Rev B 1987, 35, 197.
24. Balberg, I. Trends Stat Phys 1998, 2, 39.
25. Balberg, I. Phys Rev B 1998, 57, 13351.
26. Stanley, H. E. J Phys A: Gen Phys 1977, 10, L211.
27. Coniglio, A. J Phys A: Gen Phys 1982, 15, 3829.
28. Chiteme, C.; McLachlan, D. S.; Balberg, I. Phys Rev B 2003, 67, 024207.
29. Park, C.; Crooks, R.; Siochi, E. J.; Harrison, J. S.; Kenik, E.; Evans, N. Nanotechnology 2003, 14, L11.
30. Lillehei, P. T.; Rouse, J.; Park, C.; Siochi, E. J. Nano Lett 2002, 2, 827.
31. Wise, K. E.; Park, C.; Siochi, E. J.; Harrison, J. S. Chem Phys Lett 2004, 391, 207.
32. Sreekumar, T. V.; Liu, T.; Kumar, S.; Ericson, L. M.; Hauge, R. H.; Smalley, R. E. Chem Mater 2003, 15, 175.
33. Jonscher, A. K. Universal Relaxation Law; Chelsea Dielectrics Press: London, 1996; Ch. 6.
34. Kilbride, B. E.; Coleman, J. N.; Fraysse, J.; Fournet, P.; Cadek, M.; Drury, A.; Huntzler, S.; Roth, S.; Blau, W. J. J Appl Phys 2002, 92, 4024.
35. Sandler, J. K. W.; Kirk, J. E.; Kinloch, I. A.; Shaffer, M. S. P.; Windle, A. H. Polymer 2003, 44, 5893.
36. Barrau, S.; Demont, P.; Peigney, A.; Laurent, C.; Lacabanne, C. Macromolecules 2003, 36, 5187.
37. Balberg, I. Private communication.
38. Park, C.; Sauti, G. Private communication.
39. Dyre, J. C.; Schroder, T. B. Rev Mod Phys 2000, 72, 873.
40. Hunt, A. G. Philos Mag B 2001, 81, 875.
41. McLachlan, D. S.; Heaney, M. Phys Rev B 1999, 60, 12746.